Inorganic Chemistry

ARTICLE

pubs.acs.org/IC

Modulation of Metal−Metal Separations in a Series of Ag(I) and Intensely Blue Photoluminescent Cu(I) NHC-Bridged Triangular Clusters

Vincent J. Catalano,* Lyndsay B. Munro, Christoph E. Strasser, and Ahmad F. Samin

Department of Chemistry, University of Nevada, Reno, Nevada 89557, United States

Supporting Information

ABSTRACT: A series of picolyl-substituted NHC-bridged triangular complexes of Ag(I) and Cu(I) were synthesized upon reaction of the corresponding ligand precursors, $[Him(CH_2py)_2]BF_4$ (**1a**), $[Him(CH_2py\text{-}3,4\text{-}(OMe)_2)_2]BF_4$ (**1b**), $[Him(CH_2py\text{-}3,5\text{-}Me_2\text{-}4\text{-}OMe)_2]BF_4$ (**1c**), $[Him(CH_2py\text{-}6\text{-}COOMe)_2]BF_4$ (**1d**), and $[H^{S}im(CH_2py)_2]BF_4$ (**1e**), with Ag_2O and Cu_2O, respectively. Complexes $[Cu_3(im(CH_2py)_2)_3](BF_4)_3$ (**2a**), $[Cu_3(im(CH_2py\text{-}3,4\text{-}(OMe)_2)_2)_3](BF_4)_3$ (**2b**), $[Cu_3(im(CH_2py\text{-}3,5\text{-}Me_2\text{-}4\text{-}OMe)_2)_3](BF_4)_3$, (**2c**), $[Ag_3(im(CH_2py\text{-}3,4\text{-}(OMe)_2)_2)_3](BF_4)_3$, (**3b**), $[Ag_3(im(CH_2py\text{-}3,5\text{-}Me_2\text{-}4\text{-}OMe)_2)_3](BF_4)_3$ (**3c**), $[Ag_3(im(CH_2py\text{-}6\text{-}COOMe)_2)_3](BF_4)_3$ (**3d**), and $[Ag_3(^{S}im(CH_2py)_2)_3](BF_4)_3$ (**3e**) were easily prepared by this method. Complex **2e**, $[Cu_3(^{S}im(CH_2py)_2)_3](BF_4)_3$, was synthesized by a carbene-transfer reaction of **3e**, $[Ag_3(^{S}im(CH_2py)_2)_3](BF_4)_3$, with CuCl in acetonitrile. The ligand precursor **1d** did not react with Cu_2O. All complexes were fully characterized by NMR, UV−vis, and luminescence spectroscopies and high-resolution mass spectrometry. Complexes **2a**−**2c**, **2e**, and **3b**−**3e** were additionally characterized by single-crystal X-ray diffraction. Each metal complex contains a nearly equilateral triangular M_3 core wrapped by three bridging NHC ligands. In **2a**−**2c** and **2e**, the Cu−Cu separations are short and range from 2.4907 to 2.5150 Å. In the corresponding Ag(I) system, the metal−metal separations range from 2.7226 to 2.8624 Å. The Cu(I)-containing species are intensely blue photoluminescent at room temperature both in solution and in the solid state. Upon UV excitation in CH_3CN, complexes **2a**−**2c** and **2e** emit at 459, 427, 429, and 441 nm, whereas in the solid state, these bands move to 433, 429, 432, and 440 nm, respectively. As demonstrated by ^1H NMR spectroscopy, complexes **3b**−**3e** are dynamic in solution and undergo a ligand dissociation process. Complexes **3b**−**3e** are weakly photoemissive in the solid state.

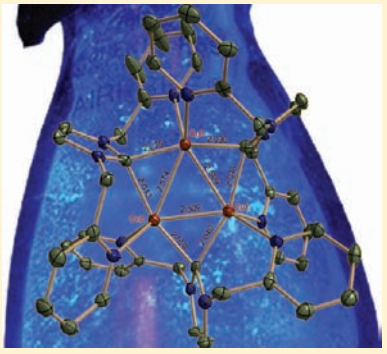

INTRODUCTION

N-heterocyclic carbenes (NHCs) are excellent ligands for transition metals, and ever since the isolation of the stable, free NHC ligands by Arduengo and co-workers[1] in 1991, NHCs have found widespread application in transition-metal chemistry, particularly in catalysis.[2−9] The NHC complexes of Ag(I) are incredibly simple to prepare and routinely employed as convenient carbene-transfer reagents.[5,10,11] Yet, on their own, Ag(I) NHC complexes are receiving increased attention because of their application as antimicrobial agents.[2,5,12] In contrast, copper(I) NHC complexes are much less prevalent in the literature but are starting to gain interest through their application in catalysis, for example, hydrosilylation,[7] dipolar cycloaddition, and [8] C−N/O[8,9] and C−C bond formation.[3,4,9]

Because of their excellent sigma-donating ability and the ease with which the precursors can be structurally modified with additional functional groups, NHCs are also ideal ligands for maintaining multimetallic architectures, producing complexes with short metal−metal interactions.[5,9,11] These noncovalent, attractive (metallophilic) interactions are often responsible for luminescence frequently observed in compounds of the group 11 metals.[13−17] While aurophilic attractions between Au(I) centers are the most well-studied,[18−21] the metallophilic interactions of the lighter coinage metals Cu and Ag remain less explored.[22−25]

In 2003, we reported the structure and luminescent properties of the NHC-bridged trimetallic complex, $[Ag_3(im(CH_2py)_2)_3](BF_4)_3$, containing a nearly equilateral Ag_3^{3+} triangular core with very short Ag···Ag separations ranging from 2.7598(8) to 2.7765(8) Å (Scheme 1).[26] Despite the Coulombic repulsion between the cationic Ag(I) centers, the observed intermetallic separations are considerably shorter than the sum of the van der Waals radii and even shorter than the Ag···Ag distance found in the bulk metal (2.889 Å).[27] Likewise, a similar Ag···Ag separation was found in the analogous 2-quinolyl-substituted NHC complex, $[Ag_3(im(CH_2quin)_2)_3](BF_4)_3$.[28] This triangular $[Ag_3L_3]^{3+}$ arrangement appears to be a common structural motif in silver-NHC chemistry, and a number of other groups have reported similar complexes. Youngs and co-workers[29] found Ag···Ag separations of 2.7869(6)−2.8070(5) Å in the hydroxymethyl-substituted complex, $[Ag_3(im(CH_2py\text{-}6\text{-}CH_2OH)_2)_3](NO_3)_3$, whereas Lee[30] and co-workers observed Ag···Ag separations ranging from 2.8182(5) to 2.8312(5) Å in the closely related

Received: May 18, 2011
Published: August 08, 2011

Scheme 1

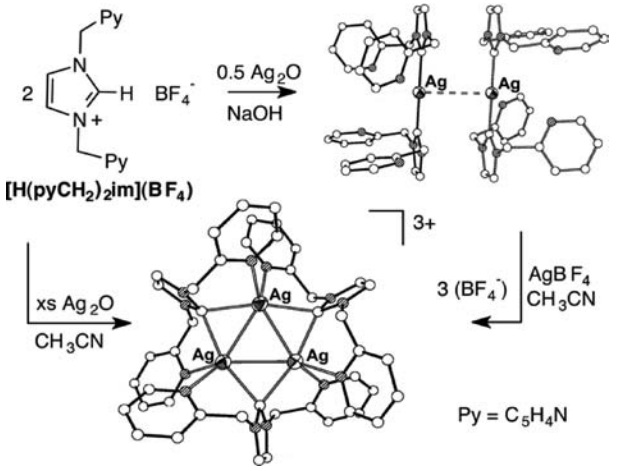

Scheme 2

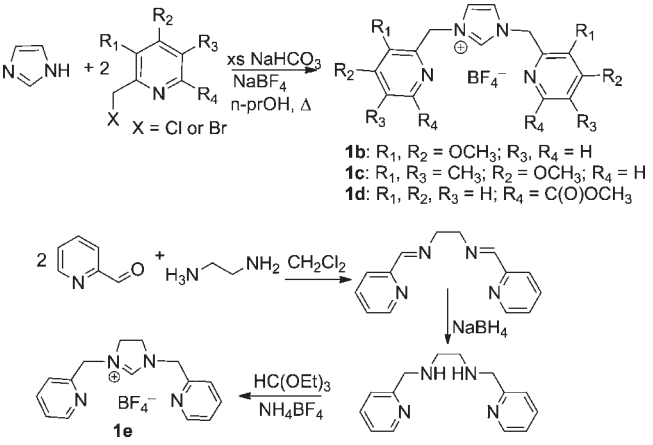

Scheme 3

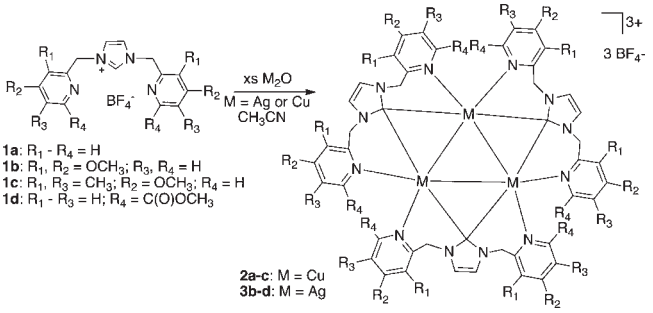

methyl-substituted complex, $[Ag_3(im(CH_2py\text{-}6\text{-}Me)_2)_3](PF_6)_3$. Extending the NHC backbone, Chen and co-workers[31] prepared the benzimidazole-NHC-based triangular Ag_3 complex, $[Ag_3(benzim\text{-}(CH_2py)_2)_3](BF_4)_3$, that contains very short Ag···Ag separations of only 2.777(1) Å. Finally, the triangular $[Ag_3L_3]^{3+}$ motif is not limited to symmetrically substituted NHC ligands. In 2005, we reported[32] the structure of $[Ag_3(MeimCH_2py)_3(MeCN)_2]\text{-}(BF_4)_3$ (MeimCH$_2$py = 1-methyl-3-[(2-pyridyl)methyl]imidazol-2-ylidene), which also contains a Ag_3^{3+} triangular core bridged by the dissymmetric bidentate MeimCH$_2$py ligand with Ag···Ag separations ranging from 2.7598(8) to 2.7832(8) Å. Two of the three silver centers are coordinated by additional acetonitrile molecules that occupy the remaining coordination sites resulting from the lack of a second picolyl donor group on the NHC ligand. The role of ligand constraint in these short separations can be discounted because the $im(CH_2py)_2$ ligand is capable of spanning metal−metal separations as long as 4.6 Å[33] and as short as 2.49 Å, as demonstrated in this work.

The Cu(I) NHC chemistry is still relatively unexplored[34] compared to that of Ag(I) even though the applicability of Cu(I) NHC molecules to catalysis has been demonstrated.[3,4,7−9] The analogous NHC-bridged $[Cu_3L_3]^{3+}$ triangular complexes are conspicuously absent from the literature. Only recently, two examples of related copper complexes with less flexible linker-free 1,3-bis(2-pyrimidinyl)imidazolylidene ligands have been reported.[35] There are, however, reports of other structural motifs exhibiting short intermetallic contacts between Cu(I) or Ag(I) with NHC ligands bearing pyridyl functional groups. For example, tri- and tetranuclear copper and silver NHC complexes showing short intermetallic distances are known for linear,[36−39] butterfly, or rectangular[37,40−42] arrangements of the metal atoms. There also exists an extensive body of literature on triangular d^{10} complexes bridged by anionic pyrazolate ligands;[43−50] however, in these cases, the metal−metal separations are typically greater than 3 Å.

In this Article, we present an extended study on NHC-bridged triangular complexes of Cu(I) and Ag(I) where we explore the modulation of the intermetallic distances by steric and electronic effects and its implication on the luminescent behavior.

RESULTS

As shown in Scheme 2, the imidazole-based NHC ligand precursors **1b**−**1d** were prepared analogously to the previously reported[51] imidazolium salts, **1a**, by simple alkylation of imidazole with the respective (halomethyl)pyridine. The imidazolinylidene-based NHC precursor **1e** was prepared analogously to literature procedures[52,53] by first condensing 1,2-diaminoethane with pyridine-2-carboxaldehyde to form a Schiff base that was then reduced with $NaBH_4$. The resulting secondary amine was cyclized with triethyl orthoformate in the presence of NH_4BF_4 to yield the imidazolinium salt.

According to Scheme 3, the triangular carbene compounds **2a**−**2c** were conveniently prepared by stirring the respective ligand precursor with an excess of Cu_2O in refluxing acetonitrile. The corresponding silver complexes, **3b**−**3d**, were prepared at room temperature analogously to the preparation of **3a**.[26] Likewise, as shown in Scheme 4, the saturated NHC precursor **1e** $[H^Sim(CH_2py)_2]BF_4$ reacts smoothly at room temperature with excess Ag_2O to form $[Ag_3(^Sim(CH_2py)_2)_3](BF_4)_3$, **3e**. The corresponding reaction with Cu_2O failed, and $[Cu_3(^Sim(CH_2py)_2)_3](BF_4)_3$, **2e**, could only be obtained through a transmetalation reaction[54] of the silver analog with CuCl. All attempts to prepare the Cu(I) triangular complex with the ester-containing ligand precursor **1d** failed. The direct reaction with Cu_2O did not produce any metalated product, and the transmetalation of **3d** with copper halide yielded only impure, multimetallic mixtures.

All of these metal complexes dissolve readily in common organic solvents, including acetonitrile, acetone, and dichloromethane, except for **2c** and **3c**, which are nearly insoluble in chlorocarbons. The copper compounds are air-stable in solution and in the solid state. The analogous silver compounds do not noticeably decompose when protected from ambient light.

dx.doi.org/10.1021/ic201053t |Inorg. Chem. 2011, 50, 8465–8476

Scheme 4

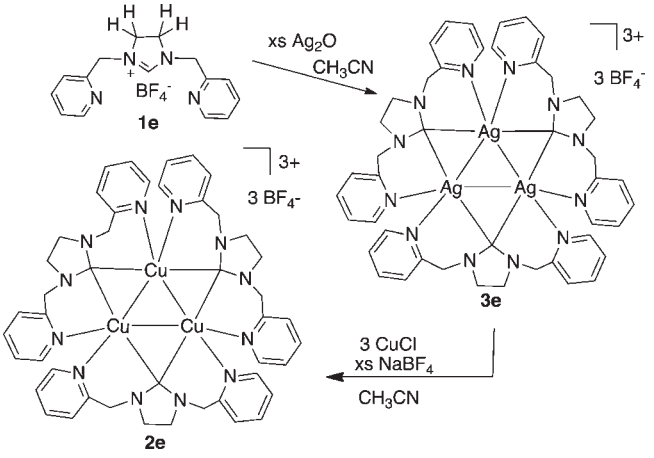

Crystals suitable for single-crystal X-ray diffraction were obtained for complexes **2a**−**2c**, **2e**, and **3b**−**3e**. Crystals of **2b**·6.5CH_3CN grown from acetonitrile and diethyl ether contained significant solvent disorder and yielded poor data. Its structure is provided in the Supporting Information (Figure S3). Better quality crystals were obtained by slow vapor diffusion of Et_2O into propionitrile solutions of **2b**. Crystallographic details are listed in Table 1. Comparative views of the cationic portions of the copper-containing species **2a**−**2c** and **2e** are presented in Figure 1, while complete thermal ellipsoid plots and bond distances and angles are provided in the Supporting Information. Selected bond distances and angles for **2a** and **2b** are listed in Table 2, whereas distance and angle data for **2c** and **2e** are provided in Tables 3 and 4, respectively.

As seen in Figure 1, the copper-containing cations are nearly D_3 symmetric with a triangular Cu_3 core wrapped by three NHC ligands. Each Cu(I) center is coordinated by two pyridyl groups and two bridging NHC moieties from alternating ligands. The methylene linkages of the same NHC ligand are positioned to opposite faces of the Cu_3 core. Both **2a** and **2b** crystallize in the monoclinic space group $P2_1/c$ each with a complete cation in the asymmetric unit, whereas complex **2c** crystallizes in the monoclinic space group $C2/c$ with only one-half of the cation in the asymmetric unit. The remaining atoms of the cation are related by a crystallographic 2-fold rotation. Complex **2e** crystallizes in the trigonal space group $R3$, and only one-third of the complex is crystallographically unique with the remaining atoms related by 3-fold symmetry.

The metal−metal separations in **2a**−**2c** and **2e** are very similar and remarkably short. As shown in Table 2, the Cu−Cu separations range from 2.5088(8) to 2.5143(7) Å for the unsubstituted pyridyl complex, **2a**, and these distances are quite similar to the values (2.5014(5)−2.5150(5) Å) in the dimethoxy-substituted pyridyl-containing complex, **2b**. The shortest separations, albeit not by much, are found in the mixed dimethylmethoxy−pyridyl-substituted complex, **2c**, where the Cu1−Cu2 and Cu2−Cu2A distances measure only 2.4907(10) and 2.5054(12) Å. Saturating the imidazole backbone has very little effect on the Cu−Cu distances, and metal−metal separation measures 2.4929(7) Å in the highly symmetric complex, **2e**. Likewise, there is little variance in the Cu−C and Cu−N separations in **2a**−**2c** and **2e**; however, the average Cu−N distances do roughly track the trend in metal−metal separations.

Table 1. X-ray Crystallographic Data for 2a−2c, 2e, and 3b−3e

compound	**2a**·0.5CH_3CN	**2b**·3C_2H_5CN	**2c**·3CH_2Cl_2	**2e**·3CH_3CN	**3b**·4C_2H_5CN·$C_4H_{10}O$	**3c**·C_2H_5CN·$C_4H_{10}O$	**3d**·CH_3CN	**3e**·4CH_3CN
formula	$C_{45}H_{42}Cu_3N_7B_3F_{12}$·0.5$C_2H_3N$	$C_{57}H_{66}Cu_3N_{12}O_{12}B_3F_{12}$·3$C_3H_3N$	$C_{63}H_{78}Cu_3N_{12}O_6B_3F_{12}$·3$CH_2Cl_2$	$C_{45}H_{48}Cu_3N_{12}B_3F_{12}$·3$C_2H_3N$	$C_{57}H_{66}Ag_3N_{12}O_{12}B_3F_{12}$·4$C_2H_3N$·$C_4H_{10}O$	$C_{63}H_{78}Ag_3N_{12}O_6B_3F_{12}$·$C_3H_5N$·$C_4H_{10}O$	$C_{57}H_{54}Ag_3N_{12}O_{12}B_3F_{12}$·$C_2H_3N$	$C_{45}H_{48}Ag_3N_{12}B_3F_{12}$·4$C_2H_3N$
fw	1222.5	1727.5	1805.2	1331.2	1933.6	1812.6	1724.2	1505.2
crystal size, mm	0.02 × 0.02 × 0.02	0.23 × 0.12 × 0.04	0.22 × 0.05 × 0.02	0.15 × 0.04 × 0.02	0.10 × 0.05 × 0.04	0.18 × 0.17 × 0.03	0.22 × 0.03 × 0.03	0.15 × 0.12 × 0.04
crystal system	monoclinic	monoclinic	monoclinic	trigonal	monoclinic	trigonal	trigonal	trigonal
space group	$P2_1/c$	$P2_1/c$	$C2/c$	$R3$	$P2_1/c$	$P3_1$	$P\bar{3}1c$	$P31c$
a, Å	11.5777(5)	12.0260(1)	13.1899(7)	12.9314(2)	28.9522(5)	12.5762(1)	13.4196(3)	13.0585(3)
b, Å	35.4318(15)	26.5274(3)	20.8644(11)	12.9314(2)	13.0597(2)	12.5762(1)	13.4196(3)	13.0585(3)
c, Å	12.3604(6)	24.3308(2)	28.1272(16)	31.0630(6)	22.8804(4)	42.7806(4)	19.9460(5)	21.1922(5)
β, °	91.321(4)°	99.161(1)°	100.510(2)		110.102(1)			
V, Å^3	5069.1(4)	7662.97(12)	7610.7(7)	4498.47(13)	8124.2(2)	5859.71(9)	3110.75(13)	3129.63(13)
Z	4	4	4	3	4	3	2	2
ρ, Mg·m^{-3}	1.602	1.497	1.575	1.474	1.581	1.541	1.841	1.597
μ, mm^{-1}	1.340	0.922	1.129	1.140	0.813	0.833	1.046	1.015
R_1 [$I > 2\sigma(I)$]	0.0509	0.0548	0.0682	0.0531	0.0532	0.0379	0.0564	0.0373
wR_2 (all data)	0.1136	0.1712	0.2100	0.1632	0.1343	0.0740	0.1359	0.1154

dx.doi.org/10.1021/ic201053t |*Inorg. Chem.* 2011, 50, 8465–8476

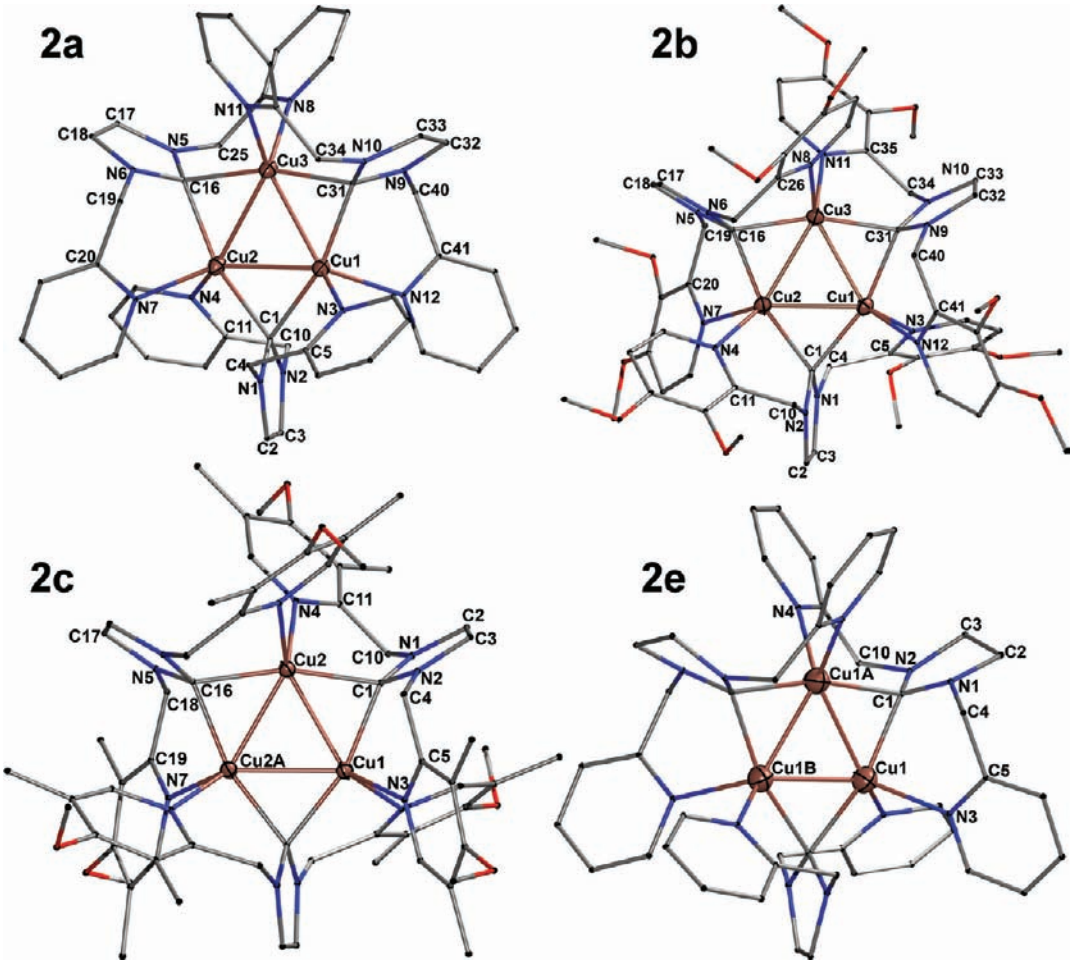

Figure 1. X-ray crystallographic drawings of the cationic portions of **2a**−**2c** and **2e**. All but the metal atoms are represented as small spheres. Hydrogen atoms are not shown for clarity. Complete thermal ellipsoid drawings and bond distances and angles are presented in the Supporting Information (Figures S1−S5).

The shortest Cu−N_{ave} at 2.141 Å is found in **2c**, followed very closely by **2b** where Cu−N_{ave} is 2.143 Å. The two complexes without auxiliary pyridyl-substitutions (**2a** and **2e**) have similar, yet slightly longer, Cu−N_{ave} separations of 2.155 and 2.151 Å, respectively. The Cu_3 cores of **2a**−**2c** possess nearly equilateral angles close to 60°, whereas in **2e**, the core is crystallographically restrained to an equilateral triangle. In all of the copper-containing complexes, the N_{py}−Cu−N_{py} angles, which range from 91 to 98°, are more reflective of a cis coordination mode, while the $C_{carbene}$−Cu−$C_{carbene}$ angles are distorted from linearity and range from 162.2(1)° to 164.8(1)°.

Crystallographic data for the Ag(I)-containing triangular species, **3b**−**3e**, are presented in Table 1. Both **3b** and **3c** crystallize with one complete cation in the asymmetric unit, whereas **3d** and **3e** possess 3-fold symmetry and crystallize with only one-third of the cation in the asymmetric unit. Structural diagrams of **3b**−**3e** are presented in Figure 2, while complete thermal ellipsoid plots and bond distances and angles are presented in the Supporting Information. Selected bond distances for **3b** and **3c** are presented in Table 5, whereas Tables 6 and 7 list selected distances and angles for **3d** and **3e**, respectively. Like their copper congeners, the cations of **3b**−**3e** all contain equilateral (or nearly equilateral) Ag_3 cores wrapped by three NHC ligands. The bridging carbene moieties position themselves nearly perpendicularly to the trimetallic face, forcing the pendant picolyl groups to either side of the Ag_3 core. Like its copper counterpart, the shortest Ag−Ag separation is found in the dimethylmethoxy−pyridyl-substituted complex, **3c**, where Ag1−Ag2, Ag1−Ag3, and Ag2−Ag3 measure only 2.7634(3), 2.7276(3), and 2.7226(3) Å, respectively. These values are very close to those found in the saturated backbone complex, **3e**, where all three symmetry-related Ag−Ag distances measure only 2.7292(5) Å. Not surprisingly, the longest Ag−Ag separation is measured in the ester containing complex, **3d**, where this substitution in the 6-position of the pyridyl group causes significant congestion around these aryl groups. The carbonyl moiety of the ester group is directed toward the nitrogen atom of the adjacent pyridyl ring with an O−N separation of ∼3.1 Å. Figure 3 presents a larger view of this steric congestion. In the dimethoxy-substituted pyridyl complex **3b**, the Ag−Ag separations of 2.7471(6), 2.7568(6), and 2.7584(6) Å for Ag1−Ag2, Ag2−Ag3, and Ag1−Ag3, respectively, although longer than those found in **3c**, are still quite short. The average Ag−N separations roughly track the trend observed in the Ag−Ag distances. In the series, complexes **3c** and **3e** have nearly equal Ag−N_{ave} separations of 2.37 and 2.36 Å, respectively, consistent with their shorter Ag−Ag distances. The longest Ag−N distance of 2.685(4) Å is found in the ester-containing species **3d** where

dx.doi.org/10.1021/ic201053t |*Inorg. Chem.* 2011, 50, 8465–8476

Table 2. Selected Bond Lengths (Å) and Angles (°) for 2a and 2b

	2a	2b
Cu1−Cu2	2.5088(8)	2.5014(5)
Cu2−Cu3	2.5143(7)	2.5150(5)
Cu1−Cu3	2.5089(8)	2.5055(5)
C1−Cu1	2.040(4)	2.051(3)
C1−Cu2	2.030(5)	2.014(3)
C16−Cu2	2.044(5)	2.007(3)
C16−Cu3	2.026(5)	2.042(3)
C31−Cu1	2.044(4)	2.056(3)
C31−Cu3	2.033(5)	2.039(3)
Cu1−N3	2.165(4)	2.132(3)
Cu1−N12	2.128(4)	2.139(2)
Cu2−N4	2.189(4)	2.134(3)
Cu2−N7	2.146(4)	2.158(2)
Cu3−N8	2.130(4)	2.153(3)
Cu3−N11	2.171(4)	2.143(2)
Cu1−Cu2−Cu3	59.93(2)	59.928(13)
Cu2−Cu1−Cu3	60.14(2)	60.306(14)
Cu1−Cu3−Cu2	59.93(2)	59.765(13)
Cu1−C1−Cu2	76.12(16)	75.96(10)
Cu2−C16−Cu3	76.31(17)	76.8(1)
Cu1−C31−Cu3	75.96(15)	75.44(10)
N3−Cu1−N12	91.73(15)	96.08(10)
N4−Cu2−N7	94.31(15)	92.13(10)
N8−Cu3−N11	93.36(15)	97.53(10)
C1−Cu1−C31	163.70(19)	163.45(11)
C1−Cu2−C16	163.36(18)	164.56(11)
C16−Cu3−C31	164.28(18)	162.22(11)
C4−N1−N2−C10	−34.5	27.2
C19−N5−N6−C25	−41.7	21.5
C34−N10−N9−C40	−40.5	32.1

Table 3. Selected Bond Lengths (Å) and Angles (°) for 2c[a]

Cu1−Cu2	2.4907(10)
Cu2−Cu2A	2.5054(12)
Cu1−C1	2.032(6)
Cu2−C16	2.029(6)
Cu2−C1	2.026(5)
Cu1−N3	2.129(5)
Cu2−N4	2.154(5)
Cu2−N7	2.139(5)
Cu1−Cu2−Cu2A	59.806(18)
Cu2−Cu1−Cu2A	60.39(4)
Cu1−C1−Cu2A	75.74(19)
Cu2−C16−Cu2A	76.2(3)
N3−Cu1−N3A	93.3(3)
N4−Cu2−N7	95.16(18)
C1−Cu1−C1A	164.4(3)
C1−Cu2−C16	163.7(2)
C10−N1−N2−C4	12.2
C18−N5−N5A−C18A	16.5

[a] Symmetry operator for atoms labeled A: $-x, y, -z + 1/2$.

Table 4. Selected Bond Lengths (Å) and Angles (°) for 2e[a]

Cu1−Cu1A	2.4929(7)
Cu1−C1	2.042(4)
Cu1−C1A	2.044(4)
Cu1−N3	2.153(4)
Cu1−N4A	2.148(4)
Cu1−Cu1A−Cu1B	60.0
Cu1−C1−Cu1A	75.20(13)
N3−Cu1−N4A	93.28(13)
C1−Cu1−C1A	164.80(13)
C4−N1−N2−C10	67.6

[a] Symmetry operator for atoms labeled A and B: (A) $-y + 1, x - y + 1$; (B) $-x + y, -x + 1, z$.

the carbonyl−pyridyl repulsion prevents closer approach of the nitrogen-containing moiety (Figure 3). The intermediate with a Ag−N_{ave} separation of 2.40 Å is **3b**.

In CD_3CN solution, the ^1H NMR spectra (Supporting Information) of the copper-containing species are consistent with their solid-state structures. The approximate D_3 symmetry is reflected in the diastereotopic methylene linkages that appear as AB quartets between 4.35 and 5.28 ppm for **2a**−**2c**. In **2e**, these methylene linker resonances are shifted upfield to 4.27 and 3.92 ppm and are joined by an AA′BB′ pattern at 3.76 and 3.55 ppm assigned to the backbone protons of the imidazolinylidene NHC ligand. The pyridyl protons in **2a** were assigned based on its 2D-ROESY, gCOSY, and gHSQC spectra, and notably, the signal of the H^6 of the pyridyl ring appears at 6.585 ppm, which is unusually shielded by 1.96 ppm relative to its ligand precursor. This diamagnetic anisotropy[55] stems from the orientation of this proton and its close proximity (2.9 Å) to the centroid of the NHC imidazole ring.[56,57] Saturating the imidazole removes the aromaticity, and hence the "ring current", and forces the H^6 signal in **2e** back downfield to 7.82 ppm even though the distance between the proton and the centroid of the imidazolinylidene remains short at ∼3.0 Å. In the dimethylmethoxy-substituted pyridyl complex **2c**, the H^6 resonance is easily identified as a singlet that appears at 6.23 ppm, whereas the corresponding proton in **2b** resonates at 6.28 ppm. Both of these complexes have short proton−$NHC_{centroid}$ separations ranging from 2.8 to 3.0 Å.

At room temperature, all of the triangular Ag_3 compounds are fluxional. As shown in Figure S19 (Supporting Information), in CD_3CN at 25 °C, the methylene protons in the dimethoxy-substituted **3b** appear as two broad resonances at 4.83 and 5.60 ppm. In the dimethylmethoxy-substituted **3c**, the corresponding resonances have coalesced to a very broad single peak at 5.12 ppm. The dynamic process in the ester-containing **3d** is more facile, and at room temperature, the methylene protons are close to the fast exchange limit, appearing as a sharp singlet 5.44 ppm. Saturating the imidazole backbone as in **3e** retards this process, but the complex is still fluxional with four broad resonances appearing at 4.57, 4.22, 3.89, and 3.62 ppm associated with the four methylene groups. This dynamic behavior is consistent with the pyridyl dissociation mechanism as is the observation that the sterically encumbered **3d** exhibits the most facile exchange. Furthermore, mixing samples of **3c** and **3e** leads to rapid ligand exchange, as evidenced by the increased number of resonances observed in the ^1H NMR spectrum. In contrast, mixing **2c** and **2e** results only in the superposition of the two spectra, indicating that there is no exchange. Likewise, addition of $[Cu(NCCH_3)_4]BF_4$ to an NMR

dx.doi.org/10.1021/ic201053t |Inorg. Chem. 2011, 50, 8465–8476

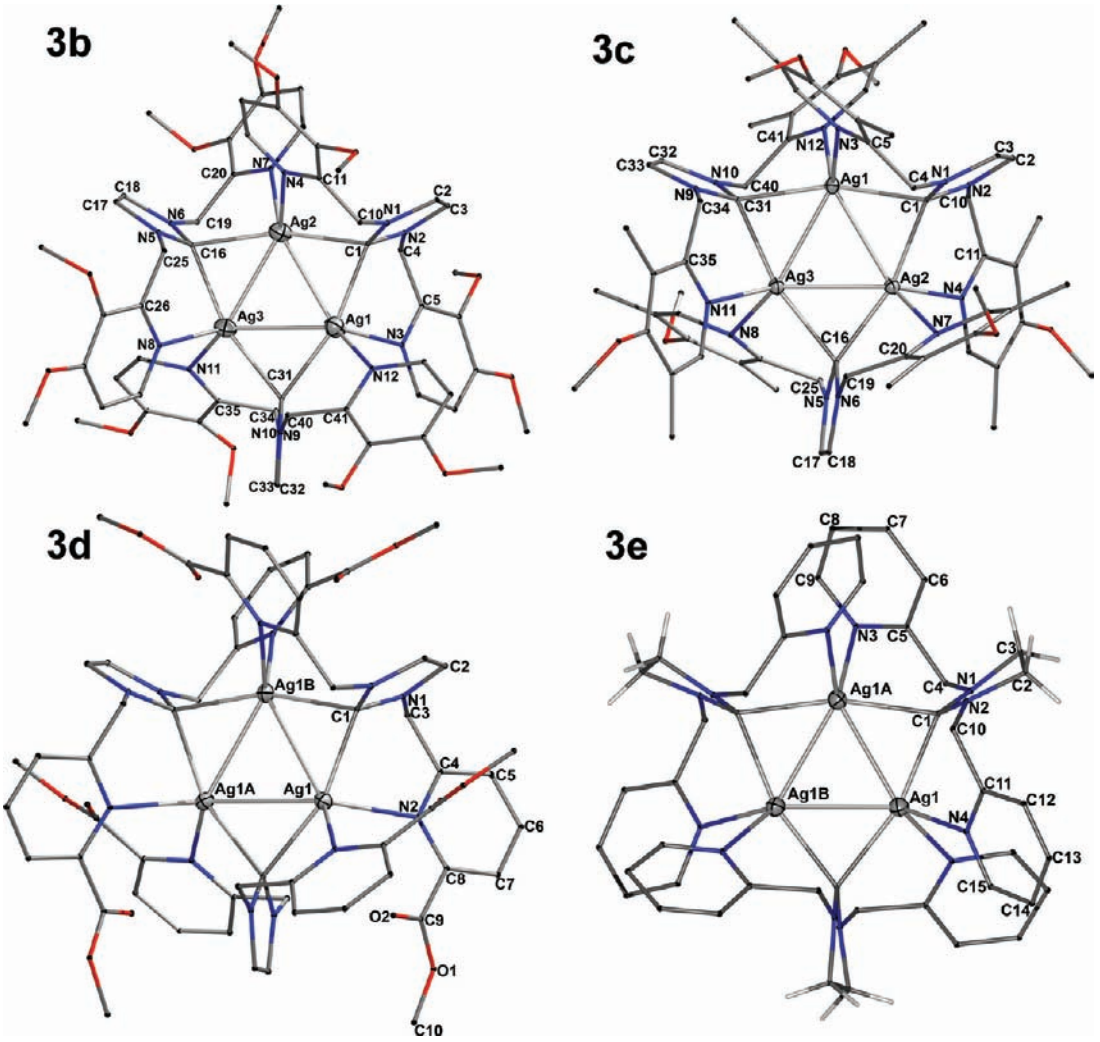

Figure 2. X-ray crystallographic drawings of the cationic portions of **3b**−**3e**. All but the metal atoms are represented as small spheres. Hydrogen atoms are not shown for clarity. Complete thermal ellipsoid drawings and bond distances and angles are presented in the Supporting Information (Figures S6−S9).

sample of **3b** nearly instantaneously generates a spectrum consistent with a mixture of Cu- and Ag-containing species.

Variable-temperature NMR data are presented in the Supporting Information (Figures S20, S24, S30), and portions of the VT NMR spectra (d_6-acetone) for **3e** and the room-temperature spectrum of **2e** are shown in Figure 4. The poor solubility of complexes **3b**−**3e** made it difficult to find a single solvent in which the complexes remain soluble at low temperature while spanning a wide enough temperature range to capture the entire dynamic process. In all cases, the stopped exchange limit exceeded the experimental conditions. Switching from d_3-acetonitrile to d_6-acetone appears to slow the dynamic process. For example, in d_6-acetone at 25 °C, the methylene resonances of **3b** now appear as a broad AB quartet that coalesces into two broad singlets near 50 °C, but this temperature is still below the fast exchange limit. Lowering the temperature regenerates the AB quartet and shifts the two pyridyl resonances downfield to 7.13 and 7.19 ppm and the NHC backbone proton to 7.95 ppm. At −85 °C, the complex starts to precipitate. A similar trend is observed for **3c**, but the process is more facile. In d_6-acetone at 25 °C, the methylene protons appear as two broad, unresolved resonances that split into an AB quartet at ∼15 °C. A similar trend is observed for the saturated ligand species **3e** (d_6-acetone) where the stopped exchange limit again exceeds the experimental conditions, but a clear pattern similar to that of **2e** is observed at −60 °C. Heating this sample to 50 °C significantly broadens the four methylene resonances but does not bring it to the fast exchange limit. The ester-containing species, **3d**, has poor solubility in acetone. In CD_3CN at −40 °C, the sharp singlet observed at room temperature corresponding to the fast exchange of the methylene protons only broadens slightly, indicating only slight diminution of the dynamic process.

The $^{13}C\{^1H\}$ spectra of **2a**−**2c**, **2e**, and **3b**−**3e** show the expected signals at shifts comparable to the ligand precursors, except for the NHC carbon signals, which are not observed in the routine 1D spectra. Only by performing gHMBC experiments could the carbene shift be determined; crosspeaks with the carbene were observed for both the CH_2 linker groups and $H^{4/5}$ of the NHC. For the silver compounds **3b** and **3c**, additional $^1J_{AgC}$ coupling constants of 96(1) and 97(2) Hz, respectively, were observed. The resolution of the 2D spectrum did not allow further analysis into ^{107}Ag and ^{109}Ag contributions or detection of

dx.doi.org/10.1021/ic201053t |*Inorg. Chem.* 2011, 50, 8465–8476

Table 5. Selected Bond Lengths (Å) and Angles (°) for 3b and 3c

	3b	3c
Ag1−Ag2	2.7471(6)	2.7634(3)
Ag2−Ag3	2.7568(6)	2.7226(3)
Ag1−Ag3	2.7584(6)	2.7276(3)
C1−Ag1	2.224(6)	2.261(3)
C1−Ag2	2.244(5)	2.218(3)
C16−Ag2	2.234(5)	2.202(3)
C16−Ag3	2.255(5)	2.261(3)
C31−Ag1	2.242(6)	2.282(3)
C31−Ag3	2.242(5)	2.277(3)
Ag1−N3	2.405(4)	2.365(3)
Ag1−N12	2.381(5)	2.352(3)
Ag2−N4	2.382(5)	2.347(3)
Ag2−N7	2.427(4)	2.436(3)
Ag3−N8	2.386(5)	2.375(3)
Ag3−N11	2.418(4)	2.360(3)
Ag1−Ag2−Ag3	60.154(15)	59.624(8)
Ag2−Ag1−Ag3	60.098(15)	59.446(8)
Ag1−Ag3−Ag2	59.748(15)	60.931(8)
Ag1−C1−Ag2	75.88(18)	76.18(9)
Ag2−C16−Ag3	75.78(18)	75.19(10)
Ag1−C31−Ag3	75.91(18)	73.48(10)
N3−Ag1−N12	99.25(15)	109.38(9)
N4−Ag2−N7	102.09(16)	100.54(9)
N8−Ag3−N11	103.95(15)	98.51(10)
C4−N1−N2−C10	−18.4	−1.9
C19−N6−N5−C25	−25.1	2.1
C34−N9−N10−C40	−28.1	0.0

additional splitting by the remaining silver nucleus not bridged by the NHC. Similar experiments for **3d** and **3e** did not reveal the Ag−C coupling.

All of the compounds were further characterized by high-resolution electrospray mass spectrometry (Figures S42−S48, Supporting Information). With the exception of **3d**, the multimetallic assemblies remain intact in the gas phase where peaks with the proper isotopomer patterns corresponding to $\{[M_3L_3](BF_4)_2\}^+$ are observed. For **3d**, only peaks corresponding to ligand precursor (**1d**) were observed.

In acetonitrile, the electronic absorption spectra of the ligand precursors **1a**−**1e** each show a single sharp band between 253 and 265 nm associated with the pyridyl $\pi-\pi^*$ transition. All but the ester-containing ligand precursor (**1d**) also show additional weak shoulders at ∼294 nm. These features are generally retained in the Cu_3-containing species along with additional peaks at 374, 366, and 373 nm for **2a**, **2b**, and **2c**, respectively. In the saturated ligand system, **2e**, this band appears blue shifted to 338 nm. As shown in Figure 5, the copper-containing triangles **2a**−**2c** and **2e** exhibit very intense, blue photoluminescence in solution. The trend in emission maxima roughly follows their substitution pattern. At room-temperature (CH_3CN), the dimethoxy-substituted **2b** and dimethylmethoxy-substituted **2c** have the most blue shifted emission maxima at 427 and 429 nm, respectively, followed by the saturated imidazole-containing complex **2e**, which emits at 441 nm under UV excitation. At 459 nm, the emission of the unsubstituted species, **2a**, is

Table 6. Selected Bond Lengths (Å) and Angles (°) for 3d[a]

	3d
Ag1−Ag1A	2.8624(9)
C1−Ag1	2.240(5)
C1−Ag1A	2.240(5)
Ag1−N3	2.685(4)
Ag1−N3B	2.685(4)
Ag1A−Ag1−Ag1B	60.0
Ag1−C1−Ag1B	79.4(2)
N3−Ag1−N32A	75.72(10)
C3−N1−N1C−C3C	−11.7

[a] Symmetry operator for atoms labeled A−C: (A) $-x+y, -x, z$; (B) $x, x-y, -z+1/2$; and (C) $-y, -x, -z+1/2$.

Table 7. Selected Bond Lengths (Å) and Angles (°) for 3e[a]

	3e
Ag1−Ag1A	2.7292(5)
C1−Ag1	2.241(6)
C1−Ag1B	2.236(6)
Ag1−N3	2.358(6)
Ag1−N4A	2.372(6)
Ag1A−Ag1−Ag1B	60.0
Ag1−C1−Ag1A	75.11(19)
N3−Ag1−N4B	95.26(18)
C10−N1−N2−C4	64.4

[a] Symmetry operator for atoms labeled A and B: (A) $-x+y, -x, z$; (B): $-y, x-y, z$.

the most red shifted. The excitation spectra (Supporting Information) for **2a**−**2c** show that these emission bands are effectively populated by two states. Changing the solvent has a negligible effect on the emission maxima, and **2b** shows no measurable change in emission maximum or peak shape in chloroform, dichloromethane, acetone, or acetonitrile. However, in the solid state, the emission maxima of **2a** shifts markedly to 433 nm, whereas only small shifts in the emission maxima are observed for **2b**, **2c**, and **2e**, which now emit at 429, 432, and 440 nm, respectively. The silver-containing triangles **3b**−**3e** are much less emissive and less well-behaved. As evidenced by their dynamic NMR spectroscopic behavior, complexes **3b**−**3e** dissociate in acetonitrile solution, and their corresponding luminescence spectroscopy is unreliable. In the solid state, only complexes **3c** and **3e** yielded reliable data with emission maxima at 425 and 424 nm, respectively. The emission spectra for solid samples of complexes **3b** and **3d** are similar with broad weak emission bands centered at ∼410 nm.

DISCUSSION

This work and the recent reports from the groups of Youngs,[29] Lee,[30] and Chen[31] and our group clearly demonstrate that picolyl-substituted NHC molecules are excellent ligands for stabilizing the triangular $[Ag_3L_3]^{3+}$ structural motif and that subtle substitutions in ligand design can lead to significant variation in Ag−Ag separation. For example, the silver triangle, $[Ag_3(im(CH_2py)_2)_3](BF_4)_3$, derived from the unsubstituted picolyl NHC ligand contains Ag(I)···Ag(I) separations ranging

dx.doi.org/10.1021/ic201053t |Inorg. Chem. 2011, 50, 8465–8476

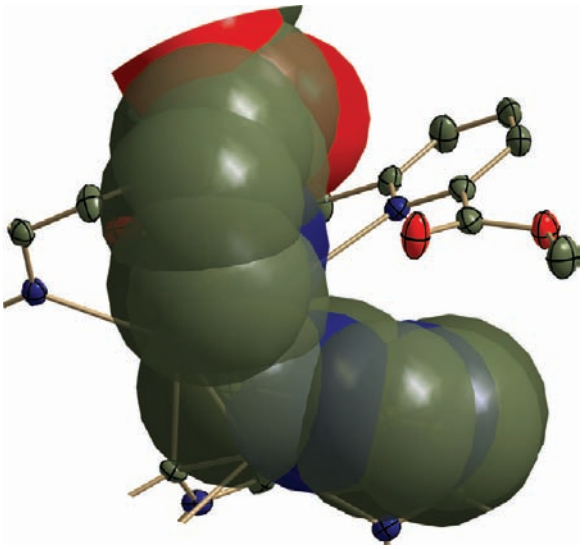

Figure 3. X-ray crystallographic representation of the steric repulsion between the methyl ester and pyridyl groups in the crystal structure of **3d**·MeCN. One ligand is shown as transparent spheres with van der Waals radii.

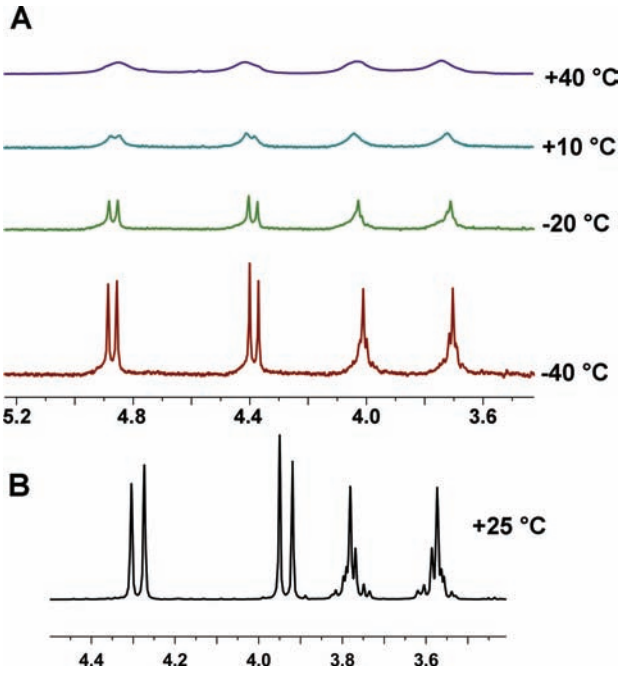

Figure 4. Part A: subset of the variable-temperature NMR spectra for the methylene region of $[Ag_3(^{S}im(CH_2py)_2)_3](BF_4)_3$ (**3e**) in d_6-acetone. Part B: room-temperature NMR data for the methylene region of $[Cu_3(^{S}im(CH_2py)_2)_3](BF_4)_3$ (**2e**) in d_3-acetonitrile.

from 2.7598(8) to 2.7765(8) Å.[26] Incorporation of a methyl group into the 6-position on the pyridyl group introduces some steric encumbrance at the pyridyl centers, preventing their close approach to the Ag center, as evidenced by the relatively long (>2.5 Å) Ag−N separation. As a consequence, the Ag···Ag separations lengthen to 2.8182(5)−2.8312(5) Å.[30] Youngs and co-workers noted a similar trend in the 6-hydroxymethyl-pyridyl-substituted NHC complex $[Ag_3(im(CH_2py\text{-}6\text{-}CH_2OH)_2)_3](NO_3)_3$ where the Ag···Ag separations are similarly lengthened

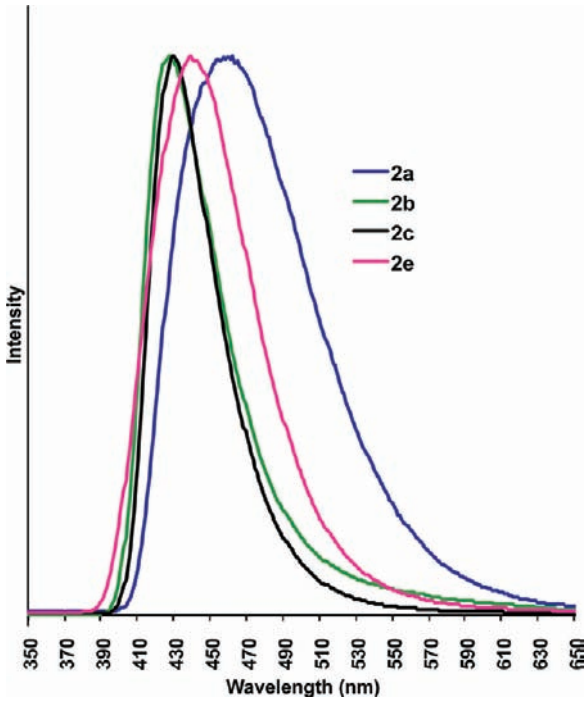

Figure 5. Normalized room-temperature emission spectra (CH_3CN) for **2a**−**2c** and **2e**.

and range from 2.7869(6) to 2.8070(5) Å].[29] This substitution is taken to an extreme in **3d** where the incorporation of a methyl ester group adds significant steric repulsion between the carbonyl and pyridyl groups. The longer Ag···Ag separations of 2.8624(9) Å are consistent with very long Ag−N_{py} separations of 2.685(4) Å. This weak ligand attachment is also manifested in VT NMR spectroscopy where the stopped exchange limit eluded detection. Such long Ag−N interactions are not frequently encountered in the literature, but a few exist. For example, comparable distances were found in a butterfly-shaped tetrametallic cluster[41] with a 1-[(1,8-naphthyridin-2-yl)methyl]-3-[(2-pyridyl)methyl]imidazolylidene (Ag−N up to 2.656 Å) and in the [tris-(2-methylphenyl)phosphine]{bis[(2-pyridyl)methyl]-amine}silver cations where the longest Ag−N distances measure 2.618 and 2.659 Å.[58,59]

The shorter Ag···Ag separations found in **3b** and **3c** ranging from ~2.72 to 2.76 Å are consistent with the addition of electron-donating groups onto the pyridyl rings, though the effect is not as dramatic as the differences seen by incorporating sterically encumbering groups. Saturated imidazole NHC ligands are not significantly better sigma donors than their unsaturated counterparts,[60] and therefore, the short Ag···Ag separation of 2.7292(5) Å measured in **3e** likely originates from geometric considerations rather than electronic.[61] The $^{S}im(CH_2py)_2$ ligand is less rigid and allows for increased flexibility of pendant picolyl side arms. This is manifested in the increased $CH_2-N-N-CH_2$ torsion angle of 64° in the $^{S}im(CH_2py)_2$-containing complex compared to 30−34° for the same measurement in the unsaturated analog, $[Ag_3(im(CH_2py)_2)_3](BF_4)_3$.[26]

To the best of our knowledge, complexes **2a**−**2c** and **2e** are the first triangular NHC-bridged $[Cu_3L_3]^{3+}$ complexes with flexible pendant arms reported. Unlike their Ag(I) congeners, these complexes are robust and substitution-inert, making them

dx.doi.org/10.1021/ic201053t |*Inorg. Chem.* 2011, 50, 8465–8476

ideal molecules for continued investigation. Complexes **2a**−**2c** are air stable and easily prepared by the simple reaction of Cu_2O with the appropriate ligand precursor. The similarly stable complex **2e** with its saturated ligand backbone could only be prepared through a transmetalation reaction with **3e** and cuprous halide. The inability to prepare the ester-containing Cu_3 complex with the ligand precursor **1d** is not unexpected given that the smaller triangular Cu_3 core relative to the Ag_3 analog would induce increased congestion around the Cu(I) centers, preventing adequate pyridyl coordination. Triangular Cu_3 complexes are abundant in the literature; however, a search of the Cambridge Crystallographic Data Centre found only a modest number of Cu_3-containing complexes with Cu−Cu separations shorter than 2.6 Å. Most relevant is the closely related $[Cu_3(impy_2)_3]^{3+}$ complex very recently prepared by Chen and co-workers[62] through a novel electrochemical procedure. Here, the Cu−Cu separations are similarly short and range from 2.465(1) to 2.497(1) Å. None of the remaining entries in the CCDC is a homoleptic complex with neutral ligands, making the short Cu···Cu separations of ∼2.5 Å found in **2a**−**2c** and **2e** particularly noteworthy. For example, Floriani and co-workers[63] reported very short Cu−Cu separations ranging from 2.44 to 2.60 Å in the mesityl-bridged $Cu_4(Mes)_4(SC_4H_8)_2$ complex. Subsequently, Jäkle and co-workers[64] reported a similar perfluorophenyl-bridged Cu_4 cluster with 2.43−2.47 Å Cu−Cu separations. Slightly longer Cu−Cu separations of 2.519 Å were reported by Hawthorne and co-workers[65] in their trinuclear "cupracarborane" complex. Yam and co-workers[66−69] have extensively explored phosphine-bridged Cu_3 complexes that are face-capped by an acetylide ligand and found Cu−Cu separations ranging from ∼2.45 to 3.27 Å. The Cu−Cu separations measured in **2a**−**2c** and **2e** follow a similar trend observed in the analogous Ag complexes where increased electron density at the pyridyl site results in a shorter Cu−Cu separation. The differences in the separations are quite small, and the shortest separations are found in the complex with the most electron-rich pyridyl substitution, **2c**, followed very closely by the dimethoxy complex, **2b**, then the saturated imidazole backbone complex, **2e**. The longest separations at ∼2.51 Å are found in the unsubstituted species.

One of the most striking features of complexes **2a**−**2c** and **2e** is their intense, blue photoemission. Although the nature of the excited state is yet undetermined, preliminary data point toward a predominantly metal cluster-centered process. The lack of any solvent effect on the emission energy is in conflict with the generation of a polar excited state typical of metal-to-ligand charge transfers; however, a delocalized and symmetrical charge-transfer process is possible. Unlike the extensively studied pyrazolate-bridged Cu_3 triangular complexes[47−50] whose close intermolecular metal−metal interactions allow for excimer formation, all of the complexes reported here have very long (>10 Å) intermolecular Cu···Cu separations in the solid state. In the absence of excited-state aggregation, the phosphorescent state of the isolated pyrazolate-bridged Cu_3 complex was assigned to a metal cluster-centered charge-transfer process mixed with some ligand-to-metal charge-transfer character.[70] Lastly, given that the ligand precursors are luminescent, an intraligand transition perturbed by the metal centers[71] is possible; however, the lack of a similar emission in the Ag_3 complexes discounts this mechanism. Regardless of the mechanism, blue emitting organometallic compounds are rare,[72−75] and this property is a highly desirable feature for efficient organometallic light-emitting diodes (OLEDs).[71,73,74,76−78] Consequently, we are currently exploring other substitutions that might influence the emission properties and give insight into the excited state along the factors that influence the material processing characteristics.

The difference in the dynamic nature of the Ag_3- and Cu_3-containing complexes is interesting. In the absence of steric congestion in the 6-postion of the pyridyl group, this dynamic behavior likely originates from the geometric differences in the metal core sizes. The smaller Cu_3 cores induce less strain across the ligand than their Ag_3 counterparts. This is evidenced by the longer intraligand $N_{py}\cdots N_{py}$ separations by ∼0.4 Å in the silver complexes relative to the copper-containing species and by the slight expansion observed in the angles around the methylene linkages in the corresponding Ag systems. The nature of the substituents in the 6-substituted pyridyl complexes is also important. In systems containing a Lewis basic heteroatom (e.g., COOMe, **3d**; and CH_2OH[29]), only a singlet for the CH_2 protons indicating fast exchange is observed, suggesting that competition for Ag coordination is possible. However, spectator substituents (benzo[28] and Me[30]) in these positions appear to freeze the dynamic motion on the NMR time scale perhaps by buttressing the ligands against each other, and sharp AB quartets are observed despite the rather long Ag−N separations, indicating a weaker pyridyl coordination. In the absence of substituents, as in $[Ag_3(im(CH_2py)_2)_3](BF_4)_3$,[26] **3b**, **3c**, and **3e**, the facile exchange process leads to single resonances. The compound $[Ag_3(benzim(CH_2py)_2)_3](BF_4)_3$[31] also shows a broad singlet, but this is likely due to the different coordination mode of the ligand and hence a different exchange phenomenon. Silver NHC complexes are expected to exhibit J_{AgC} coupling; however, such signal splitting is frequently not observed.[5] Typical $^1J_{107AgC}$ and $^1J_{109AgC}$ coupling constants for $[Ag(NHC)_2]^+$ species range from 180 to 189 Hz,[79−82] and these values are larger than those observed here. However, the bridging nature of the NHC observed in the Ag_3 triangular complexes would be expected to decrease the coupling constants. A $^1J_{109AgC}$ of 104.5 Hz was measured for the unsubstituted $[Ag_3(im(CH_2py)_2)_3](BF_4)_3$ complex,[26] which is in good agreement with the values found for **3b** and **3c**.

CONCLUSION

In this paper, we report the preparation of several new picolyl-substituted *N*-heterocyclic carbene precursors and their Cu(I)- and Ag(I)-containing triangular M_3 complexes. These eight complexes add to the growing family of NHC-bridged triangular structural motifs. Substitution away from the coordination sphere subtly influences the short M−M separations, whereas substitution at the 6-position of the pyridyl ring perturbs metal coordination in the silver-containing species, which, in turn, reduces the dispersivity at the Ag(I) center, resulting in longer Ag−Ag separations. Whereas the Ag(I) species are weakly photoluminescent at best, the Cu(I) congeners are intensely blue emissive.

EXPERIMENTAL SECTION

All chemicals were used as received. NHC precursors, **1a**[51] and **1e**,[52,53] and 2-(bromomethyl)-6-(methoxycarbonyl)pyridinium bromide[83,84] were prepared from the literature procedures. NMR spectra were measured on a Varian V500 NMR System spectrometer at the indicated frequencies and were referenced relative to the residual solvent signal. Assignments were based upon interpretation of gCOSY, gHSQC, and

gHMBC experiments. Deuterated solvents were deoxygenized by two freeze−thawing cycles for measurement of the copper compounds. Fluorescence spectra were recorded on a Jobin Yvon Horiba Fluoro-Max-3 instrument. High-resolution ESI mass spectra were obtained on an Agilent Technologies 6230 TOF-MS employing electrospray ionization in positive ion mode; required masses are calculated with ^{10}B, ^{63}Cu, and ^{107}Ag isotopes if not noted otherwise.

Single-crystal X-ray diffraction was performed on a Bruker SMART Apex CCD instrument at 100 K using graphite-monochromated Mo Kα radiation; crystals were immersed in Paratone oil and mounted on glass fibers. Data were corrected for Lorentz and polarization effects using the SAINT program and corrected for absorption using SADABS.[85,86] The structures were solved by direct methods or Patterson syntheses using the SHELXTL 6.10 software package.[87]

1,3-bis[(3,4-Dimethoxy-2-pyridyl)methyl]-1*H*-imidazolium Tetrafluoroborate ([Him(CH$_2$py-3,4-(OMe)$_2$)$_2$]BF$_4$ (1b)). Imidazole (0.587 g, 8.61 mmol), 2-(chloromethyl)-3,4-dimethoxypyridine hydrochloride (3.85 g, 17.2 mmol), and $NaHCO_3$ (3.62 g, 43.0 mmol) were added to a 100 mL round-bottom flask, and 1-propanol (40 mL) was added. The solution was refluxed overnight, cooled, and then filtered through Celite. The filtrate was evaporated to yield a pink oil, which was then taken up in 150 mL of MeOH and treated with a saturated aqueous solution of $NaBF_4$ (4.72 g, 5.44 mmol). The solution was evaporated to dryness, and the residue was taken up in CH_2Cl_2 and again filtered through Celite. The volume of the obtained solution was reduced, and a pink solid was precipitated with Et_2O in 78% yield (3.94 g). ^{1}H NMR (499.8 MHz, CD_3CN, 25 °C): δ 8.71 (m, 1H, H-2 im), 8.13 (d, J = 5.5 Hz, 2H, H-6 py), 7.42 (d, J = 1.6 Hz, 2H, H-4/5 im), 7.03 (d, J = 5.5 Hz, 2H, H-5 py), 5.44 (s, 4H, CH_2), 3.92 (s, 6H, OMe), 3.87 (s, 6H, OMe). ^{13}C NMR (125.7 MHz, CD_3CN, 25 °C): δ 159.9 (C-4 py), 147.0 (C-2 py), 146.9 (C-6 py), 144.4 (C-3 py), 137.9 (C-2 im), 124.0 (C-4/5 im), 110.0 (C-5 py), 61.6 (OMe-3), 56.9 (OMe-4), 50.6 (CH_2). MS (ESI$^+$): m/z 371.1722 [(M − BF_4)$^+$, 100%], $C_{19}H_{23}N_4O_4^+$ requires 371.171382. UV (CH_3CN) λ_{max}, nm (ε): 267 (5100).

1,3-bis[(4-Methoxy-3,5-dimethyl-2-pyridyl)methyl]-1*H*-imidazolium Tetrafluoroborate ([Him(CH$_2$py-3,5-Me$_2$-4-OMe)$_2$]BF$_4$ (1c)). The compound was prepared analogously to **1b** utilizing imidazole (0.510 g, 7.30 mmol), 2-(chloromethyl)-4-methoxy-3,5-dimethylpyridine hydrochloride (3.26 g, 14.6 mmol), $NaHCO_3$ (3.04 g, 36.2 mmol), and 1-propanol (50 mL). Compound **1c** was obtained as a colorless solid in 88% yield (2.95 g). ^{1}H NMR (499.8 MHz, CD_3CN, 25 °C): δ 8.65 (s, 1H, H-2 im), 8.13 (s, 2H, H-6 py), 7.41 (d, J = 1.6 Hz, 2H, H-4/5 im), 5.44 (s, 4H, CH_2), 3.76 (s, 6H, OMe), 2.25 (s, 6H, Me), 2.23 (s, 6H, Me). ^{13}C NMR (125.7 MHz, CD_3CN, 25 °C): δ 165.3 (C-4 py), 151.8 (C-2 py), 150.3 (C-6 py), 138.4 (C-2 im), 128.0 (C-3 py), 126.0 (C-5 py), 124.1 (C-4/5 im), 61.9 (OMe), 52.7 (CH_2), 13.5 (Me-5), 10.8 (Me-3). MS (ESI$^+$): m/z 367.2133 [(M − BF_4)$^+$, 100%], $C_{21}H_{27}N_4O_2^+$ requires 367.212853. UV (CH_3CN) λ_{max}, nm (ε): 262 (2900).

1,3-bis{[(6-Methoxycarbonyl)-2-pyridyl]methyl}-1*H*-imidazolium Tetrafluoroborate ([Him(CH$_2$py-6-COOMe)$_2$]BF$_4$, (1d)). The compound was prepared analogously to **1b** using 2-(bromomethyl)-6-(methoxycarbonyl)pyridine (3.84 g, 16.7 mmol), imidazole (0.625 g, 9.19 mmol), and $NaHCO_3$ (8.00 g, 9.52 mmol) in 100 mL of MeCN. ^{1}H NMR (499.8 MHz, CD_3CN, 25 °C): δ 8.96 (s, 1H, H-2 im), 8.06 (d, J = 7.7 Hz, 2H, H-3 py), 8.00 (t, J = 7.7 Hz, 2H, H-4 py), 7.63 (d, J = 7.7 Hz, 2H, H-5 py), 7.56 (s, 2H, H-4/5 im), 5.57 (s, 4H, CH_2), 3.88 (s, 6H, OMe). ^{13}C NMR (125.7 MHz, CD_3CN, 25 °C): δ 165.9 (COOMe), 154.3 (C-2 py), 149.1 (C-6 py), 140.0 (C-4 py), 138.3 (C-2 im), 127.0 (C-3 py), 125.8 (C-5 py), 124.3 (C-4/5 im), 54.7 (CH_2), 53.3 (OMe). MS (ESI$^+$): m/z 367.1403 [(M − BF_4)$^+$, 100%], $C_{19}H_{19}N_4O_4^+$ requires 367.140082. UV (CH_3CN) λ_{max}, nm (ε): 267 (6200).

1,3-bis[(2-Pyridyl)methyl]imidazolinium Tetrafluoroborate ([H^{S}im(CH$_2$py)$_2$]BF$_4$, (1e)). The ligand was prepared from *N*,*N*′-bis-(2-pyridyl)ethane-1,2-diamine (1.00 g, 4.13 mmol), triethyl orthoformate (0.610 g, 4.12 mmol), and NH_4BF_4 (0.671 g, 6.40 mmol), with a yield of 1.27 g (91%) of a colorless powder. ^{1}H NMR (499.8 MHz, CD_3CN, 25 °C): δ 8.68 (m, 2H, H-6 py), 8.33 (s, 1H, H-2 ^{S}im), 8.23 (m, 2H, H-4 py), 7.74 (m, 2H, H-3 py), 7.71 (m, 2H, H-5 py), 4.93 (s, 4H, pyCH_2), 3.92 (m, 4H, H-4/5 ^{S}im). ^{13}C NMR (125.7 MHz, CD_3CN, 25 °C): δ 161.1 (C-2 ^{S}im), 151.4 (C-2 py), 147.3 (C-6 py), 143.6 (C-4 py), 126.5 (C-3/5 py), 126.3 (C-5/3 py), 51.7 (CH_2), 50.3 (C-4/5 ^{S}im). MS (ESI$^+$): m/z 253.1452 [(M − BF_4)$^+$, 100%], $C_{15}H_{17}N_4^+$ requires 253.144773. UV (CH_3CN) λ_{max}, nm (ε): 255 (8500).

[Cu$_3$(im(CH$_2$py)$_2$)$_3$](BF$_4$)$_3$ (2a). Ligand precursor [Him(CH$_2$py)$_2$]-BF_4 (0.0412 g, 0.122 mmol) was refluxed with an excess of Cu_2O (0.0819 g, 0.572 mmol) in MeCN (10 mL) overnight. The suspension was filtered through Celite and reduced in volume, and a colorless powder was precipitated with Et_2O, affording 0.0441 g (90%) of a colorless solid. Crystals of **2a**·0.5MeCN suitable for X-ray diffraction were obtained by diffusion of Et_2O vapor into a MeCN solution of **2a**. ^{1}H NMR (499.8 MHz, CD_3CN, 25 °C): δ 7.95 (td, ^3J = 7.7 Hz, ^4J = 1.7 Hz, 6H, H-4 py), 7.57 (m, 6H, H-3 py), 7.42 (s, 6H, H-4/5 im), 7.22 (m, 6H, H-5 py), 6.59 (m, 6H, H-6 py), 4.91 (d, ^2J = 15.1 Hz, 6H, *H*CH), 4.80 (d, ^2J = 15.1 Hz, 6H, HC*H*). ^{13}C NMR (125.7 MHz, CD_3CN, 25 °C): δ 166.6 (*C*Cu), 151.2 (C-2 py), 147.0 (C-6 py), 137.9 (C-4 py), 123.6 (C-5 py), 123.0 (C-4/5 im), 122.7 (C-3 py), 54.0 (CH_2). MS (ESI$^+$): m/z 1111.1672 [(M − BF_4)$^+$, 0.1%], $C_{45}H_{42}B_2Cu_3F_8N_{12}^+$ requires 1111.166882. UV (CH_3CN) λ_{max}, nm (ε): 257 (120 000), 374 (25 000).

[Cu$_3$(im(CH$_2$py-3,4-(OMe)$_2$)$_2$)$_3$](BF$_4$)$_3$ (2b). The preparation followed that of **2a**. Ligand precursor [Him(CH$_2$py-3,4-(OMe)$_2$)$_2$]BF_4, **1b**, (0.159 g, 0.346 mmol) and Cu_2O (0.249 g, 1.73 mmol) afforded 0.128 g of **2b** (71%) as a tan powder. Crystals of **2b**·6.5MeCN and **2b**·3EtCN suitable for X-ray diffraction were obtained by diffusion of Et_2O vapor into MeCN or EtCN/CH_2Cl_2 solutions of **2b**, respectively. ^{1}H NMR (499.8 MHz, CD_3CN, 25 °C): δ 7.29 (s, 6H, H-4/5 im), 6.80 (d, 6H, ^3J = 6.0 Hz, H-5 py), 6.28 (d, 6H, ^3J = 6.0 Hz, H-6 py), 5.28 (d, 6H, ^2J = 15.3 Hz, *H*CH), 4.43 (d, 6H, ^2J = 15.3 Hz, HC*H*), 3.93 (s, 18H, OMe-4), 3.88 (s, 18H, OMe-3). ^{13}C{^{1}H} NMR (125.7 MHz, CD_3CN, 25 °C): δ 167.9 (*C*Cu) 157.7 (C-4 py), 144.4 (C-2 py), 143.4 (C-6 py), 140.8 (C-3 py), 122.3 (C-4/5 im), 107.7 (C-5 py), 60.8 (OMe-3), 56.2 (OMe-4), 47.7 (CH_2). MS (ESI$^+$): m/z 1471.2937 [(M − BF_4)$^+$, 0.1%], $C_{57}H_{66}B_2Cu_3F_8N_{12}O_{12}^+$ requires 1471.293609. UV (CH_3CN) λ_{max}, nm (ε): 262 (98 000), 366 (25 000).

[Cu$_3$(im(CH$_2$py-3,5-Me$_2$-4-OMe)$_2$)$_3$](BF$_4$)$_3$ (2c). Compound **2c** was prepared analogously to **2a** using **1c** (0.236 g, 0.519 mmol) and Cu_2O (0.374 g, 1.92 mmol), with a yield of 0.184 g (70%) of a colorless powder. Crystals of **2c**·3CH_2Cl_2 suitable for X-ray diffraction were obtained by evaporation of a CH_2Cl_2 solution of **2c**. ^{1}H NMR (499.8 MHz, CD_3CN, 25 °C): δ 7.35 (s, 6H, H-4/5 im), 6.23 (s, 6H, H-6 py), 4.99 (d, 6H, ^2J = 15.6 Hz, *H*CH), 4.35 (d, 6H, ^2J = 15.6 Hz, HC*H*), 3.80 (s, 18H, OMe), 2.29 (s, 18H, Me-3), 1.98 (s, 18H, Me-5). ^{13}C{^{1}H} NMR (125.7 MHz, CD_3CN, 25 °C): δ 167.7 (*C*Cu), 162.8 (C-4 py), 149.4 (C-6 py), 146.4 (C-2 py), 125.7 (C-5 py), 124.0 (C-3 py), 122.3 (C-4/5 im), 59.9 (OCH_3), 50.2 (CH_2), 13.7 (Me-5), 11.2 (Me-3). MS (ESI$^+$): m/z 1459.4156 [(M − BF_4)$^+$, 0.5%], $C_{63}H_{78}B_2Cu_3F_8N_{12}O_6^+$ requires 1459.418021. UV (CH_3CN) λ_{max}, nm (ε): 260 (48 000), 373 (8300).

[Cu$_3$(^{S}im(CH$_2$py)$_2$)$_3$](BF$_4$)$_3$ (2e). A 50 mL round-bottom flask was charged with **3e** (0.161 g, 0.11 mmol) and CH_3CN (30 mL). A solution of CuCl (34 mg, 0.35 mmol) in CH_3CN (10 mL) was added dropwise, and the mixture was stirred for 30 min. The resulting suspension was filtered through Celite, the volume was reduced, and 0.111 g (79%) of a colorless solid with a bluish tint was precipitated with Et_2O. Crystals of **2e**·3MeCN suitable for X-ray diffraction were obtained by diffusion of benzene vapor into a MeCN solution of **2e**. ^{1}H NMR (499.8 MHz, CD_3CN, 25 °C): δ 7.97 (m, 6H, H-4 py), 7.82 (m, 6H, H-6 py), 7.43 (m, 12H, H-3 and H-5 py), 4.27 (d, 6H, ^2J = 15.5 Hz, py−*H*CH), 3.92 (d, 6H, ^2J = 15.5 Hz, py−HC*H*), 3.76 (m, 6H, H-4/5 ^{S}im), 3.55 (m, 6H,

dx.doi.org/10.1021/ic201053t |*Inorg. Chem.* 2011, 50, 8465–8476

H-4/5 ^{S}im). $^{13}C\{^{1}H\}$ NMR (125.7 MHz, CD_3CN, 25 °C): δ 151.9 (C-2 py), 147.9 (C-6 py), 137.7 (C-4 py), 123.6 (C-5 py), 123.1 (C-3 py), 53.3 (py−CH_2), 50.2 (C-4/5 ^{S}im). MS (ESI^+): m/z 1117.2187 [$(M - BF_4)^+$, 0.3%], $C_{45}H_{48}B_2Cu_3F_8N_{12}^+$ requires 1117.213784. UV (CH_3CN) λ_{max}, nm (ε): 254 (110 000), 338 (18 000).

$[Ag_3(im(CH_2py\text{-}3,4\text{-}(OMe)_2)_2)_3](BF_4)_3$ (3b). A round-bottom flask was charged with **1b** (0.176 g, 0.385 mmol), Ag_2O (0.432 g, 2.18 mmol), and 30 mL of MeCN. The suspension was protected from light and stirred overnight at room temperature. Subsequent filtration through Celite, reducing in volume, and precipitation with Et_2O afforded 0.180 g of **3b** (82%) as a tan powder. Crystals of **3b**·4MeCN suitable for X-ray diffraction were obtained by diffusion of Et_2O vapor into a MeCN solution of **3b**. ^{1}H NMR (499.8 MHz, CD_3CN, 25 °C): δ 7.47 (s, 6H, H-4/5 im), 6.92 (d, 6H, ^3J = 5.8 Hz, H-6 py), 6.87 (d, 6H, ^3J = 5.8 Hz, H-5 py), 5.60 (br s, *H*CH), 4.83 (br s, HC*H*), 3.92 (s, 18H, MeO-4), 3.91 (s, 18H, MeO-3). $^{13}C\{^{1}H\}$ NMR (125.7 MHz, CD_3CN, 25 °C): δ 174.6 (t, $^1J_{CAg}$ = 96(1) Hz, CAg), 158.3 (C-4 py), 144.6 (C-6 py), 144.4 (C-2 py), 141.9 (C-3 py), 123.7 (C-4/5 im), 108.0 (C-5 py), 61.1 (OMe-3), 58.3 (OMe-4), 49.2 (CH_2). MS (ESI^+): m/z 1603.2084 [$(M - BF_4)^+$, 1%], $C_{57}H_{66}Ag_3B_2F_8N_{12}O_{12}^+$ requires 1603.220155.

$[Ag_3(im(CH_2py\text{-}3,5\text{-}Me_2\text{-}4\text{-}OMe)_2)_3](BF_4)_3$ (3c). The compound was prepared analogously to **3b** using **1c** (0.246 g, 5.41 mmol) and Ag_2O (0.623 g, 2.71 mmol), affording 0.183 g (60%) of a colorless powder. Crystals of **3c**·EtCN·Et_2O suitable for X-ray diffraction were obtained by vapor diffusion of Et_2O in an EtCN/CH_2Cl_2 solution of **3c**. ^{1}H NMR (499.8 MHz, CD_3CN, 25 °C): δ 7.53 (s, 6H, H-4/5 im), 6.84 (s, 6H, H-6 py), 5.12 (br m, CH_2), 3.79 (s, 18H, OMe), 2.38 (s, 18H, Me-5), 2.03 (s, 18H, Me-3). $^{13}C\{^{1}H\}$ NMR (125.7 MHz, CD_3CN, 25 °C): δ 173.1 (t, $^1J_{CAg}$ = 97(2) Hz, CAg), 163.3 (C-4 py), 149.4 (C-2 py), 147.7 (C-6 py), 126.1 (C-5 py), 125.0 (C-3 py), 123.6 (C-4/5 im), 60.0 (OMe), 52.1 (CH_2), 13.5 (Me-3), 11.5 (Me-5). MS (ESI^+): m/z 1591.3371 [$(M - BF_4)^+$, 0.1%], $C_{63}H_{78}Ag_3B_2F_8N_{12}O_6^+$ requires 1591.344570.

$[Ag_3(im(CH_2py\text{-}6\text{-}COOMe)_2)_3](BF_4)_3$ (3d). The compound was prepared analogously to **3b** using **1d** (0.231 g, 0.508 mmol) and Ag_2O (0.588 g, 2.54 mmol), affording 0.146 g (51%) of a tan powder. Crystals of **3d**·MeCN suitable for X-ray diffraction were obtained by diffusion of Et_2O vapor into a MeCN solution of **3d**. ^{1}H NMR (499.8 MHz, CD_3CN, 25 °C): δ 7.97 (m, 6H, H-5 py), 7.90 (m, 6H, H-4 py), 7.45 (m, 6H, H-3 py), 7.33 (s, 6H, H-4/5 im), 5.44 (s, 12H, CH_2), 3.81 (s, 18H, OMe). $^{13}C\{^{1}H\}$ NMR (125.7 MHz, CD_3CN, 25 °C): δ 178.9 (CAg), 162.8 (*C*OOMe), 154.0 (C-2 py), 145.4 (C-6 py), 137.4 (C-4 py), 124.6 (C-3 py), 123.2 (C-5 py), 121.5 (C-4/5 im), 56.2 (CH_2), 52.5 (OMe).

$[Ag_3(^{S}im(CH_2py)_2)_3](BF_4)_3$ (3e). The compound was prepared analogously to **3b** using **1e** (0.30 g, 0.88 mmol) and Ag_2O (1.02 g, 4.41 mmol), affording 0.25 g (63%) of a colorless powder. Crystals of **3e**·4MeCN suitable for X-ray diffraction were obtained by diffusion of Et_2O vapor into a MeCN solution of **3e**. ^{1}H NMR (499.8 MHz, CD_3CN, 25 °C): δ 8.12 (m, 6H, H-6 py), 7.97 (td, 6H, ^3J = 7.7 Hz, ^4J = 1.7 Hz, H-4 py), 7.49 (m, 6H, H-3 py), 7.44 (m, 6H, H-5 py), 4.57 (m, 6H, py−*H*CH), 4.22 (m, 6H, py−HC*H*), 3.89 (m, 6H, N−*H*CH), 3.62 (m, 6H, N−HC*H*). $^{13}C\{^{1}H\}$ NMR (125.7 MHz, CD_3CN, 25 °C): δ 172.7 (CAg) 151.0 (C-2 py), 148.6 (C-6 py), 137.6 (C-4 py), 123.7 (C-3 py), 123.5 (C-5 py), 54.7 (pyCH_2), 50.4 (C-4/5 ^{S}im). MS (ESI^+): m/z 1249.1470 [$(M - BF_4)^+$, 0.1%], $C_{45}H_{48}Ag_3B_2F_8N_{12}^+$ requires 1249.140330.

■ ASSOCIATED CONTENT

Supporting Information. X-ray crystallographic data for the complexes in CIF format; characterization of the compounds, including NMR, mass, and optical spectra; complete X-ray structural characterization, including thermal ellipsoid plots; and tables of bond distances and angles. This material is available free of charge via the Internet at http://pubs.acs.org.

■ AUTHOR INFORMATION

Corresponding Author
*E-mail: vjc@unr.edu.

■ ACKNOWLEDGMENT

This material is based upon work supported by the National Science Foundation under Grant No. CHE-0549902.

■ REFERENCES

(1) Arduengo, A. J.; Harlow, R. L.; Kline, M. *J. Am. Chem. Soc.* **1991**, *113*, 361.
(2) John, A.; Ghosh, P. *Dalton Trans.* **2010**, 7183.
(3) Kühl, O. *Chem. Soc. Rev.* **2007**, *36*, 592.
(4) Douthwaite, R. E. *Coord. Chem. Rev.* **2007**, *251*, 702.
(5) Garrison, J. C.; Youngs, W. J. *Chem. Rev.* **2005**, *105*, 3978.
(6) Herrmann, W. A. *Angew. Chem., Int. Ed.* **2002**, *41*, 1290.
(7) Díez-González, S.; Stevens, E. D.; Scott, N. M.; Petersen, J. L.; Nolan, S. P. *Chem.—Eur. J.* **2008**, *14*, 158.
(8) Díez-González, S.; Nolan, S. P. *Angew. Chem., Int. Ed.* **2008**, *47*, 8881.
(9) Ellul, C. E.; Reed, G.; Mahon, M. F.; Pascu, S. I.; Whittlesey, M. K. *Organometallics* **2010**, *29*, 4097.
(10) Lin, I. J. B.; Vasam, C. S. *Comments Inorg. Chem.* **2004**, *25*, 75.
(11) Lin, I. J. B.; Vasam, C. S. *Coord. Chem. Rev.* **2007**, *251*, 642.
(12) Kascatan-Nebioglu, A.; Panzner, M. J.; Tessier, C. A.; Cannon, C. L.; Youngs, W. J. *Coord. Chem. Rev.* **2007**, *251*, 884.
(13) Tiekink, E. R. T.; Kang, J.-G. *Coord. Chem. Rev.* **2009**, *253*, 1627.
(14) Gimeno, M. C.; Laguna, A. *Chem. Soc. Rev.* **2008**, *37*, 1952.
(15) Yam, V. W.-W.; Cheng, E. C.-C. *Chem. Soc. Rev.* **2008**, *37*, 1806.
(16) Fernández, E. J.; Laguna, A.; López-de-Luzuriaga, J. M. *Dalton Trans.* **2007**, 1969.
(17) Balch, A. L. *Gold Bull.* **2004**, *37*, 45.
(18) Schmidbaur, H.; Schier, A. *Chem. Soc. Rev.* **2008**, *37*, 1931.
(19) Pyykkö, P. *Inorg. Chim. Acta* **2005**, *358*, 4113.
(20) Pyykkö, P. *Angew. Chem., Int. Ed.* **2004**, *43*, 4412.
(21) Hermann, H. L.; Boche, G.; Schwerdtfeger, P. *Chem.—Eur. J.* **2001**, *7*, 5333.
(22) Carvajal, M. A.; Alvarez, S.; Novoa, J. J. *Chem.—Eur. J.* **2004**, *10*, 2117.
(23) O'Grady, E.; Kaltsoyannis, N. *Phys. Chem. Chem. Phys.* **2004**, *6*, 680.
(24) Poblet, J.-M.; Bénard, M. *Chem. Commun.* **1998**, 1179.
(25) Fernández, E. J.; López-de-Luzuriaga, J. M.; Monge, M.; Rodríguez, M. A.; Crespo, O.; Gimeno, M. C.; Laguna, A.; Jones, P. G. *Inorg. Chem.* **1998**, *37*, 6002.
(26) Catalano, V. J.; Malwitz, M. A. *Inorg. Chem.* **2003**, *42*, 5483.
(27) Liu, L.-g.; Bassett, W. A. *J. Appl. Phys.* **1973**, *44*, 1475.
(28) Catalano, V. J.; Malwitz, M. A.; Etogo, A. O. *Inorg. Chem.* **2004**, *43*, 5714.
(29) Garrison, J. C.; Tessier, C. A.; Youngs, W. J. *J. Organomet. Chem.* **2005**, *690*, 6008.
(30) Kim, G. Y.; Jung, H. J.; Park, G.; Lee, D.-H. *Bull. Korean Chem. Soc.* **2010**, *31*, 1739.
(31) Zhang, X.; Gu, S.; Xia, Q.; Chen, W. *J. Organomet. Chem.* **2009**, *694*, 2359.
(32) Catalano, V. J.; Moore, A. L. *Inorg. Chem.* **2005**, *44*, 6558.
(33) Strasser, C. E.; Catalano, V. J. *J. Am. Chem. Soc.* **2010**, *132*, 10009.
(34) Lin, J. C. Y.; Huang, R. T. W.; Lee, C. S.; Bhattacharyya, A.; Hwang, W. S.; Lin, I. J. B. *Chem. Rev.* **2009**, *109*, 3561.

(35) Chen, W.; Liu, B. *Faming Zhuanli Shenqing Gongkai Shuomingshu* **2010**, CN101787542.
(36) Liu, B.; Xia, Q.; Chen, W. *Angew. Chem., Int. Ed.* **2009**, *48*, 5513.
(37) Ye, J.; Jin, S.; Chen, W.; Qiu, H. *Inorg. Chem. Commun.* **2008**, *11*, 404.
(38) Xi, Z.; Zhang, X.; Chen, W.; Fu, S.; Wang, D. *Organometallics* **2007**, *26*, 6636.
(39) Liu, B.; Chen, W.; Jin, S. *Organometallics* **2007**, *26*, 3660.
(40) Garrison, J. C.; Simons, R. S.; Tessier, C. A.; Youngs, W. J. *J. Organomet. Chem.* **2003**, *673*, 1.
(41) Zhang, X.; Xi, Z.; Liu, A.; Chen, W. *Organometallics* **2008**, *27*, 4401.
(42) Zhou, Y.; Chen, W. *Organometallics* **2007**, *26*, 2742.
(43) Yang, C.; Elbjeirami, O.; Gamage, C. S. P.; Dias, H. V. R.; Omary, M. A. *Chem. Commun.* **2011**, *47*, 7434.
(44) Rawashdeh-Omary, M. A.; Rashdan, M. D.; Dharanipathi, S.; Elbjeirami, O.; Ramesh, P.; Dias, H. V. R. *Chem. Commun.* **2011**, *47*, 1160.
(45) Burini, A.; Mohamed, A. A.; Fackler, J. P., Jr. *Comments Inorg. Chem.* **2003**, *24*, 253.
(46) Yang, G.; Raptis, R. G. *Inorg. Chem.* **2003**, *42*, 261.
(47) Masciocchi, N.; Moret, M.; Cairati, P.; Sironi, A.; Ardizzoia, G. A.; La Monica, G. *J. Am. Chem. Soc.* **1994**, *116*, 7668.
(48) Dias, H. V. R.; Diyabalanage, H. V. K.; Rawashdeh-Omary, M. A.; Franzman, M. A.; Omary, M. A. *J. Am. Chem. Soc.* **2003**, *125*, 12072.
(49) Dias, H. V. R.; Diyabalanage, H. V. K.; Eldabaja, M. G.; Elbjeirami, O.; Rawashdeh-Omary, M. A.; Omary, M. A. *J. Am. Chem. Soc.* **2005**, *127*, 7489.
(50) Grimes, T.; Omary, M. A.; Dias, H. V. R.; Cundari, T. R. *J. Phys. Chem. A* **2006**, *110*, 5823.
(51) Magill, A. M.; McGuinness, D. S.; Cavell, K. J.; Britovsek, G. J. P.; Gibson, V. C.; White, A. J. P.; Williams, D. J.; White, A. H.; Skelton, B. W. *J. Organomet. Chem.* **2001**, *617*−*618*, 546.
(52) Ng, C.; Sabat, M.; Fraser, C. L. *Inorg. Chem.* **1999**, *38*, 5545.
(53) Vieille-Petit, L.; Luan, X.; Mariz, R.; Blumentritt, S.; Linden, A.; Dorta, R. *Eur. J. Inorg. Chem.* **2009**, 1861.
(54) Sabiah, S.; Lee, C.-S.; Hwang, W.-S.; Lin, I. J. B. *Organometallics* **2010**, *29*, 290.
(55) Martin, N. H.; Allan, N. W.; Moore, K. D.; Vo, L. *J. Mol. Struct.: THEOCHEM* **1998**, *454*, 161.
(56) Ray, M.; Ghosh, D.; Shirin, Z.; Mukherjee, R. *Inorg. Chem.* **1997**, *36*, 3568.
(57) Garces, F. O.; King, K. A.; Watts, R. J. *Inorg. Chem.* **1988**, *27*, 3464.
(58) Effendy; Marchetti, F.; Pettinari, C.; Skelton, B. W.; White, A. H. *Inorg. Chim. Acta* **2007**, *360*, 1424.
(59) Di Nicola, C.; Effendy; Marchetti, F.; Pettinari, C.; Skelton, B. W.; White, A. H. *Inorg. Chim. Acta* **2007**, *360*, 1433.
(60) Dorta, R.; Stevens, E. D.; Scott, N. M.; Costabile, C.; Cavallo, L.; Hoff, C. D.; Nolan, S. P. *J. Am. Chem. Soc.* **2005**, *127*, 2485.
(61) Winkelmann, O. H.; Riekstins, A.; Nolan, S. P.; Navarro, O. *Organometallics* **2009**, *28*, 5809.
(62) Liu, B.; Zhang, Y.; Xu, D.; Chen, W. *Chem. Commun.* **2011**, *47*, 2883.
(63) Meyer, E. M.; Gambarotta, S.; Floriani, C.; Chiesi-Villa, A.; Guastini, C. *Organometallics* **1989**, *8*, 1067.
(64) Sundararaman, A.; Lalancette, R. A.; Zakharov, L. N.; Rheingold, A. L.; Jäkle, F. *Organometallics* **2003**, *22*, 3526.
(65) Kang, H. C.; Do, Y.; Knobler, C. B.; Hawthorne, M. F. *J. Am. Chem. Soc.* **1987**, *109*, 6530.
(66) Yam, V. W.-W.; Fung, W. K.-M.; Cheung, K.-K. *Chem. Commun.* **1997**, 963.
(67) Yam, V. W.-W.; Lo, K. K.-W.; Wong, K. M.-C. *J. Organomet. Chem.* **1999**, *578*, 3.
(68) Yam, V. W.-W.; Lam, C.-H.; Cheung, K.-K. *Inorg. Chim. Acta* **2001**, *316*, 19.
(69) Yam, V. W.-W.; Lo, W.-Y.; Lam, C.-H.; Fung, W. K.-M.; Wong, K. M.-C.; Lau, V. C.-Y.; Zhu, N. *Coord. Chem. Rev.* **2003**, *245*, 39.
(70) Hu, B.; Gahungu, G.; Zhang, J. *J. Phys. Chem. A* **2007**, *111*, 4965.
(71) Yam, V. W.-W.; Wong, K. M.-C.; Hung, L.-L.; Zhu, N. *Angew. Chem., Int. Ed.* **2005**, *44*, 3107–3110.
(72) Liao, S.-H.; Shiu, J.-R.; Liu, S.-W.; Yeh, S.-J.; Chen, Y.-H.; Chen, C.-T.; Chow, T. J.; Wu, C.-I. *J. Am. Chem. Soc.* **2009**, *131*, 763.
(73) Rausch, A. F.; Thompson, M. E.; Yersin, H. *J. Phys. Chem. A* **2009**, *113*, 5927.
(74) Chang, C.-F.; Cheng, Y.-M.; Chi, Y.; Chiu, Y.-C.; Lin, C.-C.; Lee, G.-H.; Chou, P.-T.; Chen, C.-C.; Chang, C.-H.; Wu, C.-C. *Angew. Chem., Int. Ed.* **2008**, *47*, 4542.
(75) Yang, C.-H.; Cheng, Y.-M.; Chi, Y.; Hsu, C.-J.; Fang, F.-C.; Wong, K.-T.; Chou, P.-T.; Chang, C.-H.; Tsai, M.-H; Wu, C.-C. *Angew. Chem., Int. Ed.* **2007**, *46*, 2418.
(76) Bhansali, U. S.; Polikarpov, E.; Swensen, J. S.; Chen, W.-H.; Jia, H.; Gaspar, D. J.; Gnade, B. E.; Padmaperuma, A. B.; Omary, M. A. *Appl. Phys. Lett.* **2009**, *95*, 233304.
(77) Develay, S.; Blackburn, O.; Thompson, A. L.; Williams, J. A. G. *Inorg. Chem.* **2008**, *47*, 11129.
(78) Fernández, E. J.; Laguna, A.; López-de-Luzuriaga, J. M. A.; Olmos, M. E.; Pérez, J. *Chem. Commun.* **2003**, 1760.
(79) Arduengo, A. J.; Dias, H. V. R.; Calabrese, J. C.; Davidson, F. *Organometallics* **1993**, *12*, 3405.
(80) Wang, H. M. J.; Lin, I. J. B. *Organometallics* **1998**, *17*, 972.
(81) Bildstein, B.; Malaun, M.; Kopacka, H.; Wurst, K.; Mitterböck, M.; Ongania, K.-H.; Opromolla, G.; Zanello, P. *Organometallics* **1999**, *18*, 4325.
(82) Baker, M. V.; Brown, D. H.; Haque, R. A.; Skelton, B. W.; White, A. H. *Dalton Trans.* **2004**, 3756.
(83) Mato-Iglesias, M.; Roca-Sabio, A.; Pálinkás, Z.; Esteban-Gómez, D.; Platas-Iglesias, C.; Tóth, É.; de Blas, A.; Rodríguez-Blas, T. *Inorg. Chem.* **2008**, *47*, 7840.
(84) Zeng, X.; Coquière, D.; Alenda, A.; Garrier, E; Prangé, T.; Li, Y.; Reinaud, O.; Jabin, I. *Chem.—Eur. J.* **2006**, *12*, 6393.
(85) *SAINT: Program for data reduction*, version 7.68A; Bruker AXS: Madison, WI, 2009.
(86) Sheldrick, G. M. *SHELXTL: Structure Determination Software Suite*, version 6.10; Bruker AXS: Madison, WI, 2001.
(87) Sheldrick, G. M. *Acta Crystallogr., Sect. A* **2008**, *64*, 112.